

Irradiation of myoglobin by intense, ultrashort laser pulses

Juliah J. Chelliah¹ · S. V. K. Kumar¹ · Aditya K. Dharmadhikari¹ · Jayashree A. Dharmadhikari² · Deepak Mathur¹

Received: 4 July 2016 / Accepted: 6 September 2016 / Published online: 22 September 2016
© Springer-Verlag Berlin Heidelberg 2016

Abstract We probe the interaction of myoglobin with intense, femtosecond laser pulses. Significant spectral differences are found between native and the irradiated myoglobin. These arise from the disruption of the heme prosthetic group: geometrical restructuring results in alteration of the oxidation state of Fe (from its initial +3 state) which is found to be reversible on timescales of ~4–6 h. Measurements taken upon addition of OH scavengers establish the key role played by these radicals in the overall dynamics. Myoglobin remains intact upon intense field irradiation, demonstrating the structural robustness of the polypeptide backbone. Experiments utilizing intense, ultrashort laser pulses are expected to open new horizons for following, with high sensitivity, changes in the oxidation state, chemical environment, and electronic state of biomolecules in the aqueous phase.

1 Introduction

It is known that the total protein concentration in a living cell is of the order of 15 % [1]. Hence, upon exposure of a cell to ionizing radiation, the protein component is also expected to be affected along with other cell constituents. The biological effect of such radiation is, of course, predominantly determined by dosage, but the type of radiation seems to also play an essential role [2]. Over the last six

decades, it has been established that the precursor of radiation-induced damage can be either terrestrial or extraterrestrial in origin. Cosmic rays constitute the main extraterrestrial culprit; collisions of these energetic particles with constituents of the earth's upper atmosphere give rise to a gamut of energetic daughter products that induce deleterious effects on living tissue. Beams of particles from accelerators and reactors are terrestrial examples, giving rise to the formation of energetic secondary particles or high-energy electromagnetic radiation, X-rays, and gamma rays; these also induce deleterious effects on living tissue. There is, of course, naturally occurring radioactivity—both terrestrial and extraterrestrial—that also constitutes a biohazard for living matter. Within this scenario, proteins are generally damaged through the generation of free radicals that are produced due to low-energy transfer radiation (LET) [3]. LET has, consequently, become a most useful parameter for representing radiation quality along with parameters like particle energy and atomic number [4]. Considerable work has been accomplished on how, at different values of LET, the formation of free radicals leads to radiation-induced damage and the consequent modification of living matter. In the case of proteins, the basic radiolytic effects may be classified as polymer backbone degradation, cross-link formation, modification of amino acid residue radicals, change in the protein's conformation and its degree of crystallinity, oxidative degradation (when in the presence of O₂), and damage caused to one of the active sites in the enzymes [3, 5].

Recently, radiation-induced damage to living matter has also begun to be investigated using high-intensity laser pulses of ultrashort (femtosecond) duration. Ready availability of sources of ultrashort pulses of near-infrared laser light has, in the course of the last few years, enabled investigations to be made of how such pulses propagate through

✉ S. V. K. Kumar
svkk@tifr.res.in

¹ Tata Institute of Fundamental Research, 1 Homi Bhabha Road, Mumbai 400 005, India

² Department of Atomic and Molecular Physics, Manipal University, Manipal 576 104, India

various condensed media, with the motivation for such studies involving basic science [6–8] as well as a plethora of potential applications like remote sensing [9, 10] and remote control [11] of atmospheric chemistry, broadband spectroscopy [12, 13], material modification [14–17], and bond-selective chemistry [18]. The potential for applications has now started infringing upon the domain of the life sciences [19]: ultrashort, intense laser pulses have been utilized to noninvasively monitor stress-related proteins in human saliva [20] and to conduct dental and eye surgery [21]. Damage induced by intense ~30-fs-long pulses of laser light has recently been demonstrated in biomolecules—like DNA—kept under physiological conditions [22–25], and it has been suggested that detrimental dose distributions within tissue that are irradiated by gamma radiation—one of the major difficulties in radiotherapy—might be avoided by use of femtosecond laser pulses [24]. This is mainly due to the possibility of spatially confining ultrashort infrared laser pulses to volumes (~125 μm^3) that are very much smaller than what is attainable with contemporary clinical radiation sources. The significantly smaller laser–matter interaction volumes have important implications for radiation therapy (less collateral damage to healthy tissue) and in applications like multiphoton microscopy (enhanced image contrast and resolution). It has been suggested that 800-nm laser pulse-induced filamentation might yield essentially the same radiation dosage in the radiolysis of water as that obtained using very energetic gamma radiation [26].

We have explored the radiolysis of water upon irradiation by ultrashort, intense pulses of laser light, and to this end, we report here results of experiments that we have conducted on a prototypical protein, myoglobin. Quite unexpectedly, we discover that even at the high values of optical field employed in our experiments, myoglobin does not undergo fragmentation. It does, however, exhibit interesting and potentially important alterations in some properties, such as conformational changes that manifest themselves in changes in oxidation state of the Fe atom in the heme protein, as is discussed in the following. We know of no earlier reports on interactions of intense laser pulses with proteins, especially in the physiologically important aqueous phase.

2 Experimental method

We irradiate myoglobin in water using 40-fs-long pulses of intense 800-nm laser light. In our experiments, the laser pulses were loosely focused such that typical peak intensities were in the 10^{12} W cm^{-2} range. This intensity estimate is consistent with the following observation. Upon laser irradiation of the sample (myoglobin + water) kept

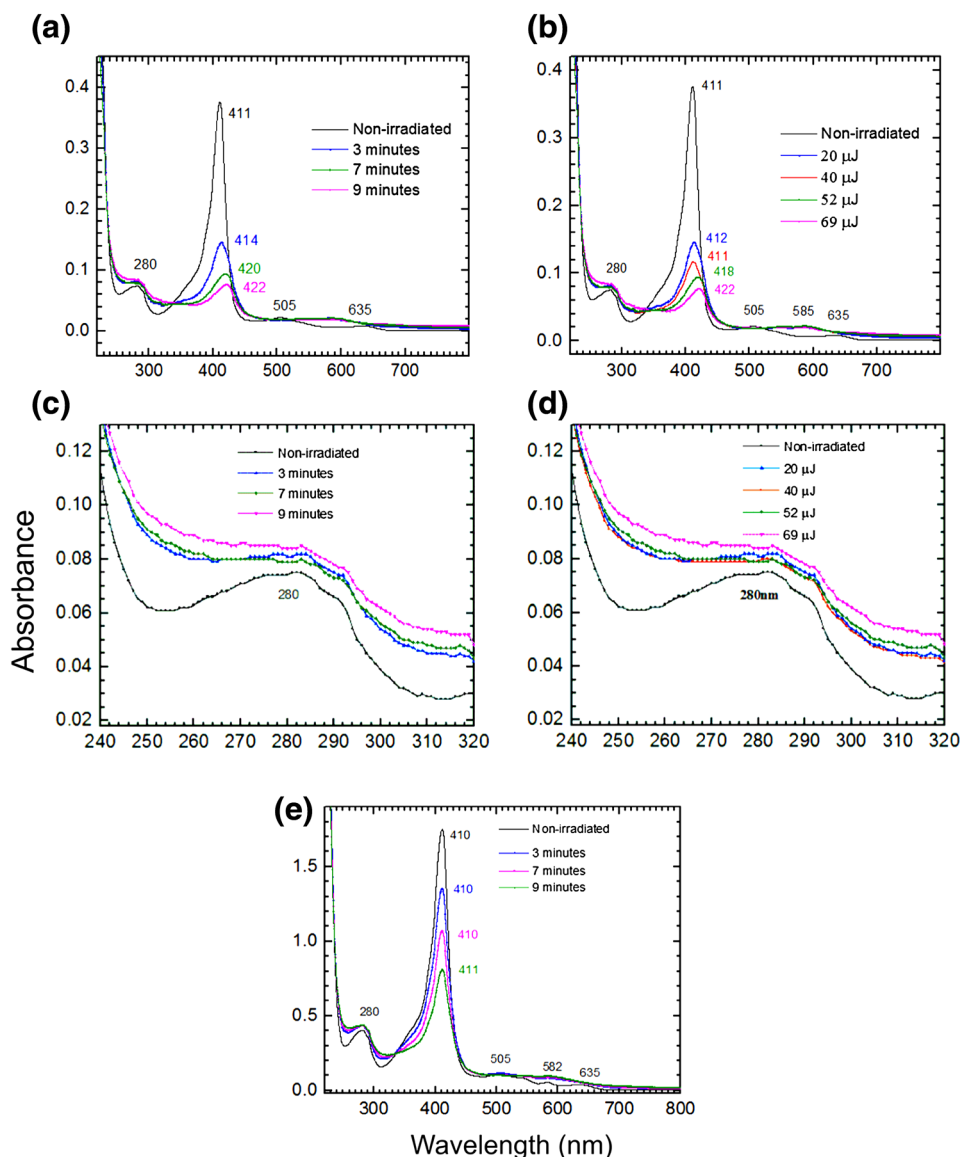
in a 1-cm-long cuvette, bubble formation was observed. It is known that the intensity threshold for bubble formation upon exposure to femtosecond pulses of 800-nm laser light is 5×10^{12} W cm^{-2} in pure water [27] and possibly marginally lower when myoglobin is suspended in water. The optical field corresponding to such intensity values is a fraction of the Coulombic field that bonds atoms and molecules; it is large enough to induce multiple ionization and, potentially, subsequent fragmentation of the irradiated protein.

The laser we used in these experiments was an amplified Ti:sapphire system producing 800-nm pulses of 40-fs duration (1 kHz repetition rate) at energies up to 1 mJ. The methodology adopted for our present set of experiments on myoglobin + water is essentially the same as those used in earlier work with water as a solvent [20, 28]. Although the laser light (800-nm wavelength) is not directly absorbed by myoglobin + water, as recent work from our laboratory has indicated, multiphoton and strong-field effects play the role of initiating the ionization–dissociation dynamics of water [22, 23], giving rise to the formation of electrons and OH radicals from the water precursor. Equine skeletal myoglobin (Sigma-Aldrich, India) was purified using PD10 columns and prepared in aqueous solution (0.5 mM) using autoclaved milliQ water. Samples placed in a 1-cm-long cuvette were irradiated with our laser pulses for a range of values of irradiation time and incident laser energy values. Irradiated and non-irradiated myoglobin samples were subjected to analysis using a spectrophotometer, circular dichroism, SDS-PAGE analysis, and MALDI ToF mass spectrometry.

3 Results and discussion

Absorption spectra of native myoglobin (Fig. 1) show characteristic peaks at 410 nm, 505 nm, and 635 nm (Fig. 1a, b). After irradiation, a shift is to a longer wavelength, accompanied with an overall decrease in the absorbance. We attribute the wavelength shift of the Soret band to the binding of a radical species to the Fe atom via hydrogen bonding [29, 30]. This results in a change of oxidation state from the native ferric (+3) to the ferrous (+2) state [31]. Changes in absorbance observed in spectra of non-irradiated (411-nm wavelength) and irradiated Mb (at 412-, 414-, 420-, and 422-nm wavelengths) [32–35] reflect the destruction of metmyoglobin with concomitant enhancement of oxymyoglobin, deoxymyoglobin, and peroxymyoglobin, respectively [36, 37]. The decreased absorbance of the Soret band (411 nm) is a signature of the heme group being distorted upon laser irradiation. Careful perusal of the short wavelength section of our spectra (Fig. 1 c, d) also indicates differences occurring at UV wavelengths. These

Fig. 1 **a** Absorption spectra of non-irradiated and irradiated myoglobin samples at constant energy (40 μJ) and different time intervals. **b** Corresponding absorption spectra at different energy values (20–69 μJ) with constant time interval. **c** Spectra in the region of 280 nm of non-irradiated and irradiated myoglobin samples at constant energy (40 μJ) with different time intervals, and **d** corresponding at different energy values (20–69 μJ) with constant time interval. **e** Absorption spectra measured 6 h after irradiating myoglobin at constant energy (40 μJ) and different time intervals. Note that the Soret band does not shift toward longer wavelengths



spectra make clear that decrease in absorbance of the 411-nm feature is accompanied by a concomitant increase of absorbance at 280 nm when comparison is made to spectra of non-irradiated protein samples. This increase is a manifestation of the exposure of the tryptophanyl residue to the protein surface induced by the laser irradiation and shows that the protein undergoes aggregation. The spectra shown in Fig. 1e were measured 6 h after laser irradiation. The Soret band no longer shifts toward longer wavelengths as the dosage (laser irradiation time) is increased, indicating that the protein has now regained its native ferric oxidation state. It is known that such autoxidation is highly sensitive to changes in pH [38–40, 46, 48, 51], with acidic pH values facilitating the ferrous–ferric transition. We measured the pH of non-irradiated and irradiated protein samples before and after irradiation; the former had a pH of 6.3 that

gradually increased to 6.6 after irradiation. A couple of hours after irradiation, the pH again dropped to 6.3, in conformity with earlier reports that femtosecond laser pulses can make an aqueous environment acidic [41].

It is important to note that metmyoglobin ($\text{HX-Fe}^{\text{III}}$) may oxidize to a two-electron oxidation product, ferrylmyoglobin ($\bullet\text{X-Fe}^{\text{IV}} = \text{O}$) in interactions involving H_2O_2 . The spectral changes following such oxidation are very similar to what we observe in our experiments: the $\text{HX-Fe}^{\text{III}}$ spectrum exhibits absorption peaks at 505 nm and 631 nm, whereas the $\bullet\text{X-Fe}^{\text{IV}} = \text{O}$ spectrum shows peaks at 548 nm and 582 nm. However, it has long been established that such oxidation occurs efficiently at pH values between 8 and 9 [42]. In the course of our experiments, as already noted, pH values were maintained well within the range 6–7 and the formation of ferrylmyoglobin will,

consequently, have a very low probability. In general terms, ferrylmyoglobin is of biological importance as it occurs in vivo and, concomitantly, possesses an ability to stimulate oxidation of unsaturated fatty acids in lipoproteins and vesicles (see [43], and references therein). $\bullet\text{X-Fe}^{\text{IV}} = \text{O}$ spontaneously decays to $\text{HX-Fe}^{\text{III}}$; the rates at which this autoreduction occurs are species dependent and vary widely [43].

Along with changes in absorption spectra, we also noticed alterations in the color of the protein upon irradiation: the irradiated samples were green in color instead of the native brown color of metmyoglobin. The green color is attributed to the interaction of H_2O_2 with the Fe–heme complex. Hydrogen peroxide is, of course, one of the most potent oxidants; it is known to be formed when intense laser pulses propagate through water [44]. The interaction of H_2O_2 with the Fe–heme complex results in distortion of the porphyrins ring which, in turn, results in crosslink formation and, thereby, the green coloration [38, 45].

The structure of the protein is associated with its function, and any changes in it are, therefore, of considerable interest. In case of myoglobin, the heme group is surrounded by eight helices. One of myoglobin's important functions is as an oxygen-storage protein in our muscles; its oxygen-binding capacity depends on the presence of the bound prosthetic group, heme. The heme group, which is responsible for the distinctive red color of blood, is the ligand associated with myoglobin where one Fe atom is located at the center of a heterocyclic organic ring, porphyrin. When O_2 is encountered, the Fe and O_2 orbitals bond and their energies change. In quantumchemical terms, the π^* orbitals of O_2 interact with the xz and z^2 orbitals of Fe. A consequence of the π^* accepting action is that, at pH values used in our experiments, Fe changes from being in the +2 (ferrous) oxidation state to the +3 (ferric) oxidation state, enabling the Fe atom to now fit snugly into the gap in the center of the heme plane. Prior to such binding, the Fe atom is located 0.55 Å above the planar porphyrin ring. Upon binding to O_2 , the Fe atom moves closer (by 0.29 Å) toward the porphyrin ring. Under such circumstances, the structural integrity of myoglobin is enhanced; this increased “robustness” is expected to make fragmentation of the protein less likely. Although fragmentation is made less likely, it is possible that not-insubstantial conformational alterations may be occurred. At values of pH higher than 8, the above discussion does not suffice as cognizance has then to be taken of the above-noted possibility of ferrylmyoglobin formation (with Fe in the +4 oxidation state).

We monitored the conformational change of the secondary structure of the protein by means of far-UV circular dichroism (CD) spectra. Utilizing the standard reference CD method described in detail by Yang et al. [46], we take the secondary structure of irradiated myoglobin to

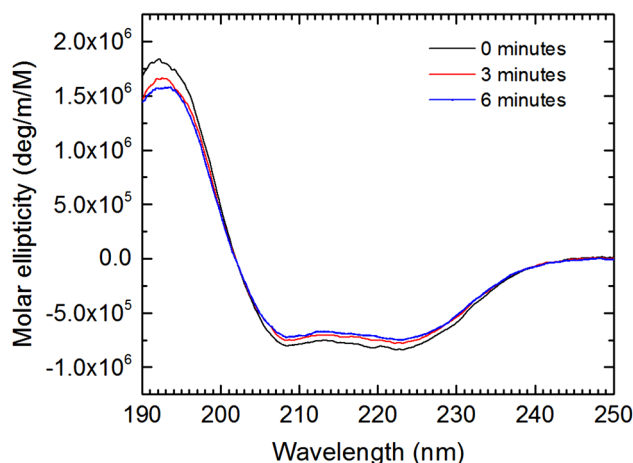


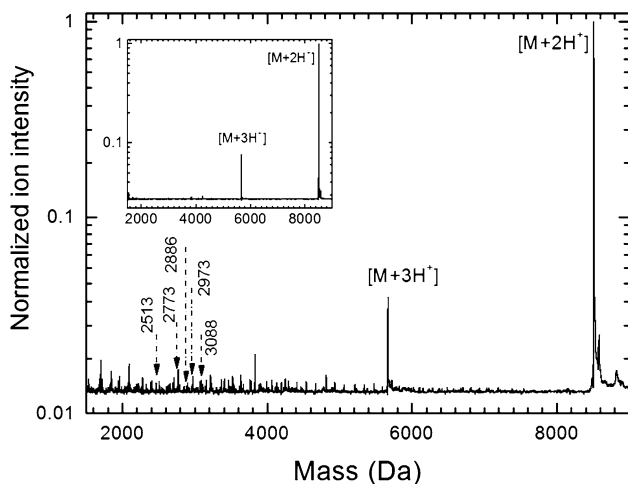
Fig. 2 Circular dichroism (CD) spectra of myoglobin irradiated with laser energy of 40 μJ for different exposure time. The spectra were measured at 25 $^\circ\text{C}$ using a 1-mm path-length cell. The spectra are the average of five scans, smoothed by polynomial curve fitting

comprise four basic structures: α -helix, β -sheets, β -turn, and random. The CD spectrum of myoglobin is then unravelled as the sum of the CD spectra of each secondary structure. Typical CD spectra of non-irradiated and irradiated myoglobin solution are shown in Fig. 2. These spectra enable estimation of the secondary structure content of irradiated myoglobin, and our results are summarized in Table 1. As has been well established since the earliest applications of the reference CD method, the accuracy associated with such estimation of secondary structure content is expected to be good in the case of myoglobin. It has been long established that there is an agreement (within 5 %) between CD-derived structural information and that deduced from X-ray diffraction measurements [47].

CD data on the irradiated protein clearly indicate a decrease in the α -helical structure when compared to the non-irradiated sample. There is concomitant increase in random coil structure. However, we note that our intense femtosecond laser pulses destabilize the α -helical structure, possibly through subsequent generation of oxygen radicals. Such destabilization of the protein structure by oxygen radicals would be expected to result in oxidative polypeptide fragmentation. We explored such possible fragmentation using mass spectrometry (with a MALDI time-of-flight spectrometer). In order to make these measurements, we dissolved 10 mg of DHB matrix in 1.0 ml of 70 % ACN: 30 % of 0.1 % TFA in water. The samples were mixed with the matrix in 1:1 ratio. One microliter of mixture was placed on a ground steel plate and allowed to dry, forming a microcrystal layer. Typical MALDI spectra of non-irradiated and irradiated proteins are shown in Fig. 3. It is noteworthy that only a very small amount of fragmentation is observed, of the order of 1–2 % compared to the doubly

Table 1 Estimation of secondary structure content of irradiated myoglobin

Exposure Conditions (min)	α -helix (%)	β -sheets (%)	β -turns (%)	Random coil (%)
0	58.8	7.8	10.7	22.7
3	54.6	17.0	5.6	22.9
6	49.9	20.0	5.4	24.7

**Fig. 3** MALDI time-of-flight mass spectra of non-irradiated (*inset*) and irradiated myoglobin samples (40 μ J, 40-fs laser pulses for 6 min). Note the total absence of peaks in the mass region 2000–3000 Da in the “background” spectrum shown in the *inset*

protonated parent peak and confined mainly to the 2500–3000 Da mass region. In view of the very low fragment ion yield that we obtain in our experiments, it is pertinent to comment on the quantitative facet of this type of mass spectrometry. Quantitative applications of MALDI encounter additional challenges over and above those faced in other mass spectrometry techniques. However, early studies carried out following the initial development of MALDI succeeded in establishing the potential of this technique

to yield reliable quantitative data in the low femtomole to attomole range for a wide variety of compounds [48].

We attribute these minor fragments in terms of bond scission between amino acids, as indicated in Table 2. The scissions that we are able to identify in our mass spectrum appear to be single-bond scissions from the carboxyl terminal. Fragment peaks in the region of 1700, 1800, and 3800 Da are also clearly discernible in the spectrum shown in Fig. 3; these are due to fragments that result from more than a single scission of the protein backbone. In order to confirm that the protein’s molecular weight remained unaltered we also carried out a SDS-PAGE analysis. The gel analysis data showed loss of staining for those protein bands which had been exposed to higher dosage [45]; no change was observed in the molecular weight of the protein.

We rationalize the above set of results by invoking laser-induced formation of free radicals. As in our earlier studies on damage to DNA induced by OH radicals that are formed upon dissociation of water that is induced by strong optical fields, the present observations are also due to the action of OH. In our experiments, we postulate that the key initiator of dynamics occurring within irradiated myoglobin is the strong optical field that is the precursor to excitation, ionization, and dissociation of H_2O , yielding species like electronically excited H_2O^* , H_2O^+ , OH, OH^* , and low-energy ionized electrons [25]. The solvated electrons have long-enough lifetimes to enable them to participate in the dynamics we describe here (estimated values of their lifetimes range from 300 ns to ~500 ps) [49, 50]. As discussed later, collisions between such electrons and water molecules can yield electronically excited states, H_2O^* , and, in turn, collisions between these H_2O^* and H_2O^+ give rise to the formation of OH radicals, $H_2O^* + H_2O^+ \rightarrow OH + H_3O^+$.

If our conjecture about the important role being played by OH radicals in inducing damage is valid, it would be expected that the effect of these radicals would be quenched upon addition of appropriate scavengers like ascorbic acid [51] or ethanol [52]. Figure 4 shows the effect that addition of one of these scavengers, ascorbic acid, has on the MALDI mass spectrum. Very similar spectra were

Table 2 Identification of fragment amino acid sequences due to single scission of myoglobin upon femtosecond laser irradiation

Mass (Da)	Bond scission between amino acids	Sequence	Type of fragmentation
2513	132–153	TKALELFRNDIAAKYELGFQG	Y
2716	130–153	AMTKALELFRNDIAAKYELGFQG	Y
2773	129–153	GAMTKALELFRNDIAAKYELGFQG	Y
2886	128–153	QGAMTKALELFRNDIAAKYELGFQG	Z
2973	127–153	AQGAMTKALELFRNDIAAKYELGFQG	Z
3088	126–153	DAQGAMTKALELFRNDIAAKYELGFQG	Z

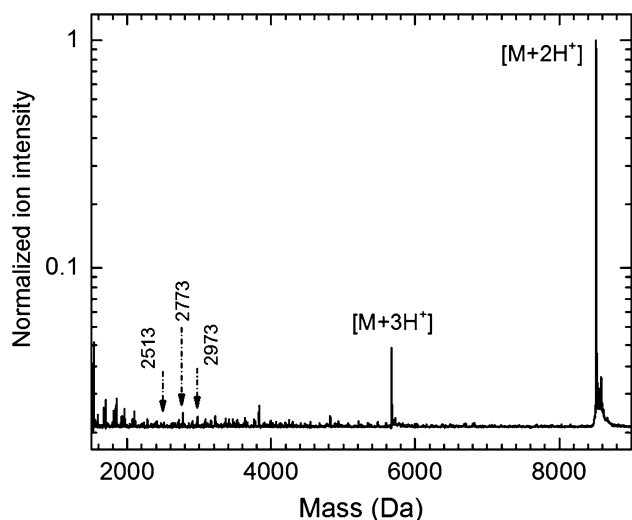


Fig. 4 MALDI time-of-flight mass spectrum of irradiated myoglobin samples (40 μ J, 40-fs laser pulses for 6 min) with the addition of the ascorbic acid, an OH scavenger

obtained upon addition of ethanol. We note that addition of ascorbic acid results in a change of pH value; our measurements offered no indications of pH-induced changes in the MALDI spectrum that might be attributable to addition of ascorbic acid.

The effects on the absorption spectra of scavengers, ascorbic acid, and ethanol were also probed. Illustrative spectra measured at constant energy (40 μ J, corresponding to an incident laser intensity of 1 TW cm^{-2}) are shown in Fig. 5. The spectra in Fig. 5 clearly establish that addition of OH scavengers permits the protein to retain its ferric oxidation state. This is most likely accomplished by shielding the Fe atom in the porphyrin ring. Furthermore, the scavengers also prevent myoglobin from undergoing aggregation. It is also interesting to note that by scavenging OH radicals from the water medium, there is no longer any possibility of H_2O_2 formation, and hence, there is a markedly decreased probability of the Fe-heme complex being destroyed. Correspondingly, the resulting green coloration formed after irradiation of myoglobin is now not observed.

In summary, our experiments have revealed that, upon irradiation of myoglobin by intense, femtosecond laser pulses, it is the laser-induced formation of OH radicals from the water medium that drives the overall dynamics that lead to alteration of the molecular properties of myoglobin. There are significant spectral differences between native and the irradiated myoglobin that arise from the disruption of the heme prosthetic group. Apart from disruption of the ordered structure of the protein, there is also evidence of crosslinking, aggregation, and degradation. Counterintuitively, there is no evidence of major fragmentation in mass spectra that we measured, demonstrating the

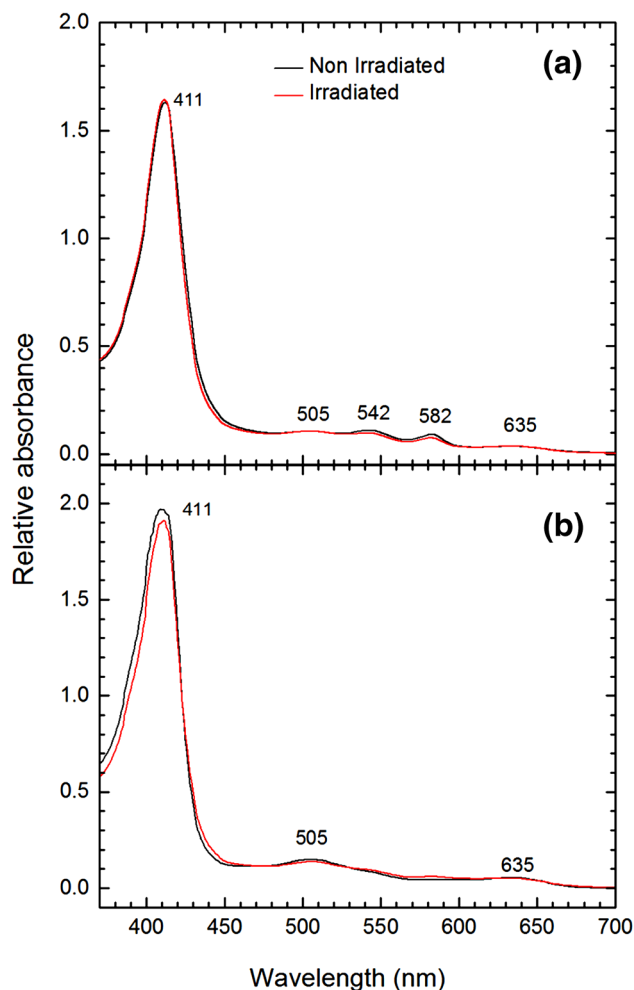


Fig. 5 Absorption spectra of non-irradiated and irradiated myoglobin with OH scavengers **a** ascorbic acid and **b** ethanol added

structural robustness of myoglobin's backbone upon irradiation by intense optical fields. The overall structural integrity of myoglobin remains intact upon intense field irradiation, but, at pH values between 6 and 7, the optical energy does lead to geometrical restructuring that gives rise to the oxidation state of Fe altering from +3 to +2. In its normal oxidation state, the Fe atom is too large to fit into the plane of protoporphyrin. Thus, the ferrous ion is located out of the porphyrin plane. However, upon oxidation to the ferric state, the loss of an electron allows the electronic charge cloud to penetrate more toward the nucleus, resulting in an overall smaller size. Thus, the iron in the ferric state is able to "fit" into the protoporphyrin plane upon attachment to O_2 .

The ferric \leftrightarrow ferrous transition is a reversible change. In our experiments, this reversibility seems to occur on time-scales of a few (\sim 4–6) hours. Measurements conducted upon addition of scavengers establish the key role played by OH radicals in the overall dynamics. The interaction of

intense laser pulses with water gives rise to the formation of a white light supercontinuum; at the intensity levels used in our experiments, the white light spectrum is expected to cover a wide wavelength range, 400–900 nm [20, 25, 28]. It is interesting to note that measurements we have made by adding scavengers also serve to indicate that the white light does not affect the dynamics which, as noted above, seem to be driven by the OH radical. We anticipate that such experiments, utilizing intense, ultrashort laser pulses, will open new horizons for following, with high sensitivity, changes in the oxidation state, chemical environment, and electronic state of biomolecules, in aqueous phase. The anticipated use of attosecond excitation in forthcoming experiments [19, 53] will make possible the imaging of biochemical processes like charge migration within diverse media of biological significance. The work that we have reported here is also likely to be of relevance in the context of femtosecond time-resolved X-ray studies on biomolecules using free-electron lasers which yield ultrafast optical excitation pulses which typically have peak power densities only somewhat smaller than those used in our experiments. The potential effect of radiation damage in such upcoming new generation of FEL experiments is an important issue [19, 54, 55]. It is also pertinent to note that results of our strong-field experiments, and forthcoming experiments carried out at FELs, will complement weak-field (single-photon) studies carried out on biomolecules using femtosecond beams of ultraviolet photons [56–59].

Acknowledgments We are grateful to Sukeert for assistance with the preliminary work using MALDI. The Department of Science and Technology is thanked for the award of the J C Bose National Fellowship to D.M. and for supporting J.A.D. under its Women Scientists Scheme. Useful discussions with Shyamalava Mazumdar on CD spectrometry are acknowledged.

References

1. J.D. Watson, *Molecular Biology of the Gene*, 2nd edn. (Saunders, Philadelphia, 1972)
2. I. Shuryak et al., *Rad. Environ. Biophys.* **48**, 275 (2010)
3. V.S. Jamwal et al., *J. Radioprotection Res.* **2**, 37 (2014)
4. M. Taguchi, T. Kojima, *Rad. Res.* **163**, 455 (2005)
5. F. Hutchison, *Ann. Rev. Nucl. Sci.* **13**, 535 (1963)
6. A. Couairon, A. Mysyrowicz, *Phys. Rep.* **441**, 47 (2007)
7. L. Bergé et al., *Rep. Prog. Phys.* **70**, 1633 (2007)
8. A. Couairon, H.S. Chakraborty, M.B. Gaarde, *Phys. Rev. A* **77**, 053814 (2008)
9. J.F. Gravel et al., *J. Anal. Chem.* **76**, 4799 (2004)
10. J. Yao et al., *Phys. Rev. A* **84**, 051802 (2011)
11. M. Rodriguez et al., *Opt. Lett.* **27**, 772 (2002)
12. S.A. Kovalenko et al., *Phys. Rev. A* **59**, 2369 (1999)
13. J. Kasparian et al., *Science* **30**, 61 (2003)
14. L.C. Courrol et al., *Opt. Exp.* **12**, 288 (2004)
15. J.A. Dharmadhikari et al., *Opt. Commun.* **284**, 630 (2011)
16. J.A. Dharmadhikari et al., *Opt. Commun.* **287**, 122 (2013)
17. J.A. Dharmadhikari et al., *Opt. Lett.* **38**, 172 (2013)
18. D. Mathur et al., *J. Chem. Phys.* **143**, 244310 (2015)
19. P. Vasa, D. Mathur, *Ultrafast Biophotonics* (Springer, Heidelberg, 2016)
20. C. Santhosh et al., *J. Biomed. Optics.* **12**, 020510–020511 (2007)
21. S.H. Chung, E. Mazur, *J. Biophoton.* **2**, 557 (2009)
22. J.S. D'Souza et al., *Phys. Rev. Lett.* **106**, 118101 (2011)
23. A.K. Dharmadhikari et al., *Phys. Rev. Lett.* **112**, 138105 (2014)
24. R. Meesat et al., *PNAS* **109**, E2508 (2012)
25. D. Mathur, *J. Phys. B.* **48**, 022001 (2015)
26. R. Meesat et al., *J. Phys: Conf. Ser.* **250**, 012077 (2010)
27. A. Vogel et al., *Appl. Phys. B* **81**, 1015 (2005)
28. P. Vasa et al., *Phys. Rev. A* **89**, 043834 (2014)
29. M. Levantino et al., *Struc. Dyn.* **2**, 041713 (2015)
30. X. Ye, A. Demidov, P.M. Champion, *J. Am. Chem. Soc.* **124**, 5914 (2002)
31. B. Livingston, *Food Technol.* **35**, 238 (1981)
32. R. Clarke, J.F. Richards, *J. Agri. Food Chem.* **19**, 170 (1971)
33. K.D. Whitburn, M.Z. Hoffman, I.A. Taub, *Rad. Phys. Chem.* **23**, 271 (1984)
34. T. Egawa, H. Shimada, Y. Ishimura, *J. Biol. Chem.* **275**, 34858 (2000)
35. F.J. Romero et al., *J. Biol. Chem.* **267**, 1680 (1992)
36. M. Chaijan, *J. Sci. Technol.* **30**, 47 (2008)
37. L. Kagen, S. Scheidt, A. Butt, *Am. J. Med.* **62**, 86 (1977)
38. G. Tajima, K. Shikama, *J. Biochem.* **25**, 101 (1993)
39. K. Shikama, *J. Am. Chem. Soc.* **98**, 1357 (1998)
40. S. Brewer, *Meat Sci.* **68**, 1 (2004)
41. S. Kohse et al., *J. Am. Chem. Soc.* **135**, 9407 (2016)
42. G.I. Tajima, K. Shikama et al., *Int. J. Biochem.* **25**, 101 (1993)
43. C. Giulivi, E. Cadenas, *Meth. Enzymol.* **233**, 189 (1994)
44. S.L. Chin, S. Lagace, *Appl. Opt.* **35**, 907 (1996)
45. J.B. Fox et al., *Agri. Food Chem.* **6**, 692 (1958)
46. J.T. Yang, C. Wu, H.M. Martinez, *Methods Enzymol.* **130**, 208 (1986)
47. G.D. Fasman, *Circular Dichroism and the Conformational Analysis of Biomolecules* (Springer, Heidelberg, 2013)
48. A. Cerpa-Poljak, A. Jenkins, M.W. Duncan, *Rapid Commun. Mass Spectrom.* **9**, 233 (1995)
49. K.J.A. Davies, *J. Biol. Chem.* **262**, 9896 (1987)
50. N.D. Nikogasyan, A.A. Oraevsky, I.V. Rupasov, *Chem. Phys.* **77**, 131 (1983)
51. R. Lian, A.R. Crowell, A.I. Shkrob, *J. Phys. Chem. A* **109**, 1510 (2005)
52. Y. Lee, K.B. Song, *J. Biochem. Molec. Biol.* **35**, 590 (2002)
53. M.P. Richard, *Antioxid Redox Sig.* **19**, 2342 (2013)
54. S.R. Leone et al., *Nature Photon.* **8**, 162 (2014)
55. T.R.M. Barends et al., *Science* **350**, 445 (2015)
56. M. Levantino et al., *Nature Commun.* **6**, 6772 (2015)
57. C. Altucci et al., *Laser Phys. Lett.* **9**, 234 (2012)
58. G. Leo et al., *Rapid Comm. Mass Spectrom.* **27**, 1660 (2013)
59. F. Itri et al., *Cell. Mol. Life Sci.* **73**, 637 (2016)